



Cite this: *Polym. Chem.*, 2018, **9**, 1571

Received 26th December 2017,

Accepted 9th February 2018

DOI: 10.1039/c7py02125a

rsc.li/polymers

Facile synthesis of advanced gradient polymers with sequence control using furan-protected maleimide as a comonomer†

Xue Gu,^a Liuqiao Zhang,^a Ying Li,^a Wei Zhang,^a Jian Zhu,^a Zhengbiao Zhang^{*a} and Xiulin Zhu^{a,b}

Gradient polymers are intriguing structures due to their unknown structure/property relationships and potential applications. Herein, advanced gradient copolymers were prepared from comonomers methyl methacrylate and furan-protected propyl maleimide (FPMI) via a reversible addition–fragmentation chain-transfer (RAFT) polymerization. During RAFT polymerization at 100 °C, propyl maleimide (PMI) was generated *in situ* from FPMI via a retro-Diels–Alder (rDA) reaction to undergo copolymerization in a gradient manner due to intrinsic reactivity ratios. At 40 °C, the rDA reaction for PMI release was not triggered. Many unprecedented gradient polymers, including simultaneous, hierarchical, di-block, symmetrical, and tri-block gradient copolymers, were successfully fabricated. Finally, the sequence-dependent thermal properties were explored. This work greatly enriches the library of gradient polymers and advances research into sequence-controlled polymerization.

Gradient copolymers are sequence-controlled polymers with compositions that gradually change from one chain end to the other. They have many attractive properties owing to their unique microstructure. For example, compared with block or random copolymers, gradient copolymers have shown distinct microphase separation,^{1–3} broad enthalpy recovery,⁴ improved polymer blend compatibilization,⁵ and special interfacial interactions.^{2,3,6,7} With the advent of controlled radical polymerization (CRP), the preparation of gradient copolymers with good chain homogeneity has become more feasible.^{1,4,7–14} In general, two methods are used to prepare gradient copolymers *via* CRP: (i) simultaneous batch copolymerization of two comonomers with inherently different reactivity ratios, which creates a simultaneous gradient and (ii) semi-batch copolymer-

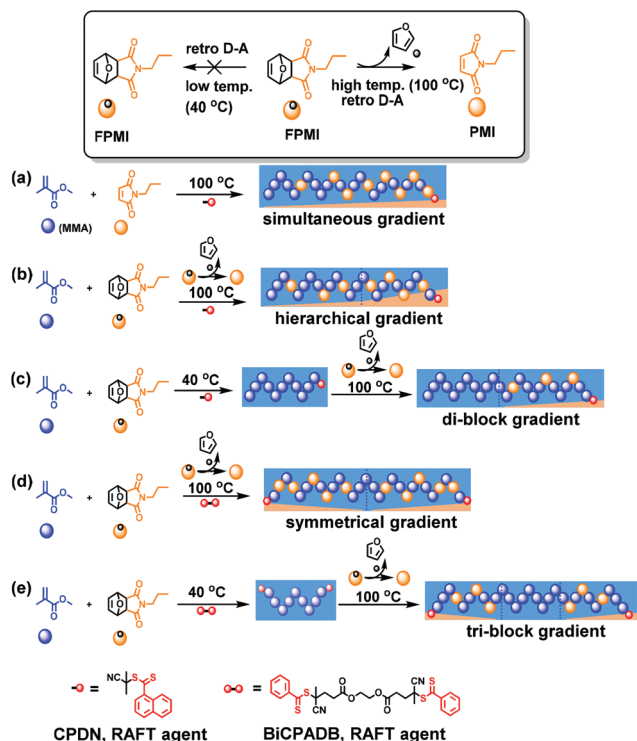
ization with continuous feeding of one comonomer, which generates a controlled (or forced) gradient.^{6,10} Using either of these two methods, a variety of gradient copolymers have been prepared from different comonomer pairs. However, gradient copolymers with advanced sequence control have yet to be widely exploited,¹⁵ despite their potential for unique and interesting properties/functions.¹⁶ To fabricate advanced gradient polymers, more sophisticated strategies are required.

Accordingly, sequence-controlled polymers have received significant attention in recent years.^{17–23} In contrast to sequence control *via* step/iterative growth polymerization,^{24–38} sequence control *via* chain growth polymerization is highly challenging due to its intrinsic mechanism. Despite this, much effort has been devoted to sequence-controlled chain polymerization, with many pioneering studies reported.^{6,33,38–63} Recently, our group has demonstrated an efficient strategy for preparing sequence-controlled polymers using furan-protected maleimide as a latent monomer.⁶⁴ This strategy relies on the temperature-dependent retro-Diels–Alder (rDA) reaction of furan and maleimide. By deliberately manipulating the temperature of styrene (St) CRP, polymerizable maleimide units can be released *via* rDA reactions and incorporated into the “living” polymer chains at customized positions. This latent monomer-based strategy provides a promising method for preparing sequence-controlled polymers.

The sequence created by chain polymerization is highly dependent on the intrinsic reactivity ratio (*r*) and feed ratio of each comonomer.⁶⁵ Alkyl methacrylate and maleimide have been reported to have *r* values of 0.833–3.22 and 0.07–0.47, respectively, depending on the specific monomer structure.^{66–72} Accordingly, simultaneous gradient copolymers have been inherently produced from the copolymerization of methyl methacrylate (MMA) and maleimide.^{73–75} By applying furan-protected maleimide as a comonomer, it is envisaged that polymerizable maleimide monomers will be increasingly released at higher temperatures *via* the rDA reaction, resulting in gradual incorporation into the growing chain. Notably, free furan cannot polymerize with MMA *via* radical polymerization, as shown by control experiments (Table S1, ESI†).

^aState and Local Joint Engineering Laboratory for Novel Functional Polymeric Materials, Jiangsu Key Laboratory of Advanced Functional Polymer Design and Application, College of Chemistry, Chemical Engineering and Materials Science, Soochow University, Suzhou 215123, China. E-mail: zhangzhengbiao@suda.edu.cn
^bGlobal Institute of Software Technology, No 5. Qingshan Road, Suzhou National Hi-Tech District, Suzhou 215163, China

†Electronic supplementary information (ESI) available. See DOI: 10.1039/c7py02125a



Scheme 1 Schematic illustration of the facile synthesis of advanced gradient copolymers by manipulating the temperature with MMA/furan-protected propyl maleimide (FPMI) as the comonomer pair: (a) simultaneous gradient, (b) hierarchical gradient, (c) di-block gradient, (d) symmetrical gradient, and (e) tri-block gradient.

Consequently, controlled (or forced) gradients can be generated. However, at lower temperatures, such as 40 °C, maleimide cannot be released; as a result, maleimide units are not incorporated into the polymer chain. Herein, for the copolymerization of MMA with furan-protected maleimide as a comonomer, the facile preparation of gradient copolymers with advanced sequence control was envisaged using controlled changes in the polymerization temperature. Gradient copolymers with advanced sequences are shown in Scheme 1. This work allows the broad design of advanced gradient copolymers, which greatly enriches the library of sequence-controlled polymers and facilitates further exploration of structure–property relationships.

Unlike the cross-propagation observed using the St–maleimide comonomer pair,⁷⁶ the MMA–maleimide comonomer pair, with r values of 0.833–3.22 and 0.07–0.47, respectively,^{66–72} resulted in gradient sequences. In this work, the MMA–furan-protected propyl maleimide (FPMI) comonomer pair was carefully selected for the fabrication of gradient copolymers with advanced sequence control. Compared with the sluggish polymerization of St at low temperatures (such as 40 °C), the polymerization of MMA had a much higher rate, even at room temperature, which made sequence-controlled polymerization more accessible. As shown in Fig. 1, the copolymerization of MMA and *N*-propyl maleimide (PMI)

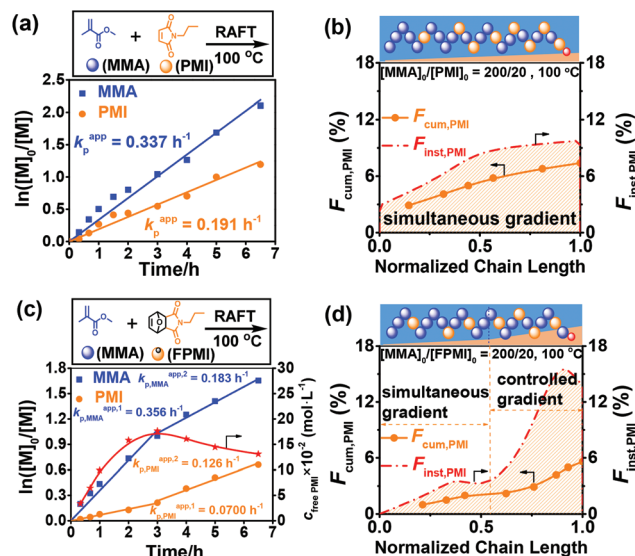


Fig. 1 Synthesis of MMA/PMI simultaneous gradient and hierarchical gradient copolymers *via* RAFT polymerization: (a) kinetic plots of MMA with PMI at 100 °C; (b) cumulative (F_{cum}) and instantaneous (F_{inst}) PMI unit contents in products as a function of normalized chain length for MMA with PMI at 100 °C; (c) kinetic plots of MMA with FPMI at 100 °C; (d) cumulative (F_{cum}) and instantaneous (F_{inst}) PMI unit contents in products as a function of normalized chain length for MMA with FPMI at 100 °C. $[MMA]_0/[PMI]_0$ or $[FPMI]_0/[CPDN]_0/[ACHN]_0 = 200/20/1/0.2$, MMA = 5.0 mL, in toluene, toluene/MMA (2/1, v/v). Normalized chain length (i) = $\text{Conv.}_{\text{total}}(i)/\text{Conv.}_{\text{max}}$; where $\text{Conv.}_{\text{max}}$ is the maximum value of $\text{Conv.}_{\text{total}}$; $F_{\text{cum,PMI}}(i) = (1 \times \text{Conv.}_{\text{PMI}})/(1 \times \text{Conv.}_{\text{PMI}} + 10 \times \text{Conv.}_{\text{MMA}})$; $F_{\text{inst,PMI}}(i - (i - 1)) = (1 \times \text{Conv.}_{\text{PMI}}(i) - 1 \times \text{Conv.}_{\text{PMI}}(i - 1))/[(1 \times \text{Conv.}_{\text{PMI}}(i) - 1 \times \text{Conv.}_{\text{PMI}}(i - 1)) + (10 \times \text{Conv.}_{\text{MMA}}(i) - 10 \times \text{Conv.}_{\text{MMA}}(i - 1))]$. The positions and numbers of both monomer unit beads are not accurate, but are provided for illustrative purposes.

was performed at 100 °C. The copolymerization was controlled *via* reversible addition–fragmentation chain-transfer (RAFT) polymerization, ensuring the “living” nature of the polymerization and the homogeneity of the generated chains. As shown in Fig. 1a, the copolymerization proceeded smoothly in a “living” fashion, as indicated by the linear kinetic plots, narrow molecular weight distributions, and increased molecular weight with the increase in conversion (Fig. S3, ESI†). The ^1H NMR spectra of the polymerization solution and recovered polymer are shown in Fig. S5 and S6 (ESI†). The changes in instantaneous PMI content ($F_{\text{inst,PMI}}$) and cumulative PMI content ($F_{\text{cum,PMI}}$) with normalized chain length were plotted (Fig. 1b). As envisaged, the polymerization of MMA with PMI produced a simultaneous gradient sequence due to the large difference in the reactivity ratio. However, when using furan-protected FPMI as a comonomer instead of naked PMI, a polymerizable PMI monomer was released gradually *via* the rDA reaction at 100 °C, and the polymerization kinetics showed a two-stage profile for both monomers (Fig. 1c). Within approximately 3.0 h, the polymerization of MMA and PMI showed linear kinetic plots, with a $k_{\text{p,MMA}}^{\text{app},1}$ of 0.356 h^{−1} and a $k_{\text{p,PMI}}^{\text{app},1}$ of 0.0700 h^{−1}, indicating that a large portion of MMA monomer was consumed by polymer-

ization. During this stage, PMI was initially released and partially incorporated into the polymer chain. The concentration of free PMI in the system was also calculated and plotted against time, as shown in Fig. 1c. The concentration of free PMI released from the rDA reaction was clearly shown to increase in the first 3.0 h of polymerization owing to PMI production from the rDA reaction being faster than its consumption. In contrast, the MMA concentration significantly decreased in the first 3.0 h due to polymerization. After 3.0 h (second stage), the concentration of free PMI (calculated from ^1H NMR spectra, as shown in Fig. S5†) decreased gradually due to the acceleration of PMI consumption ($k_{\text{p,PMI}}^{\text{app},2} = 0.126 \text{ h}^{-1}$) as the probability of cross-propagation between MMA and PMI increased ($k_{\text{p,MMA}}^{\text{app},2} = 0.183 \text{ h}^{-1}$). The two-stage polymerization profile was also confirmed by the change in $F_{\text{inst,PMI}}$ and $F_{\text{cum,PMI}}$ with normalized chain length, as shown in Fig. 1d. In the first stage, a small portion of released PMI was slowly incorporated into the polymer chain, creating a gradient. However, during the second stage, the continuous accumulation of free PMI resulted in a significant increase in PMI incorporation into the growing chains, similar to semi-batch polymerization with a continuous PMI feed. Therefore, the second stage was responsible for the controlled gradient. Overall, the polymerization of MMA with FPMI afforded a hierarchical gradient sequence, with a simultaneous gradient at the initial stage and a controlled gradient at the latter stage.

At low temperatures (such as 40 °C), the rDA reaction to release a PMI monomer cannot occur within the polymerization timescale. Therefore, polymerization at 40 °C would produce the homo-PMMA block. As shown in Fig. 2a, the polymerization of MMA and FPMI at 40 °C for 17.5 h (1st slot) created a homo-PMMA block, as denoted by the kinetic plots, with no PMI incorporation observed. This homo-PMMA block was further validated using matrix-assisted laser desorption/ionization time-of-flight (MALDI-TOF) mass spectrometry (Fig. S7†), which confirmed a sole mass gap of 100 Da (MMA unit). Afterwards, the polymerization vessel (Schlenk tube) was transferred to an oil bath prestabilized at 100 °C and allowed to react for another 6.0 h (2nd slot). At this higher temperature, MMA polymerization was significantly accelerated. Meanwhile, the rDA reaction of FPMI was triggered at high temperature, immediately releasing fresh PMI that was then slowly incorporated into the “living” chain. As shown in Fig. 2, the 2nd slot of polymerization created a gradient MMA–PMI copolymer. Therefore, by manipulating the polymerization temperature, a di-block gradient copolymer containing a homo-PMMA block and a gradient MMA–PMI block was produced. The changes in $F_{\text{inst,PMI}}$ and $F_{\text{cum,PMI}}$ with normalized chain length (Fig. 2b) clearly showed the controlled sequence of the di-block gradient copolymer. The living nature of the polymerization with the temperature jump was demonstrated using size-exclusion chromatography (SEC; Fig. 2c), which showed that the molecular weight increased with conversion. Notably, the living nature was not compromised by increasing the temperature from 40 to

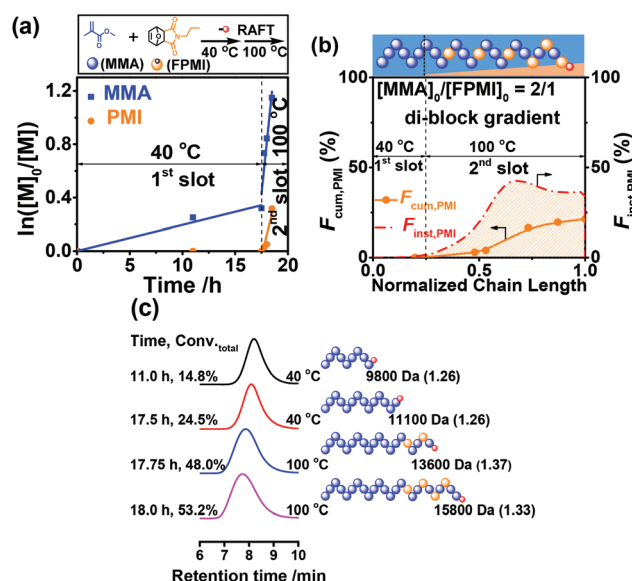


Fig. 2 Synthesis of MMA/PMI di-block gradient copolymers via RAFT polymerization: (a) kinetic plots; (b) cumulative (F_{cum}) and instantaneous (F_{inst}) PMI unit contents in products as a function of normalized chain length; and (c) SEC traces. $[\text{MMA}]_0/[\text{FPMI}]_0/[\text{CPDN}]_0/[\text{ABVN}]_0 = 200/100/1/0.5$, MMA = 3.0 mL, in DMF, DMF/MMA (2/1, v/v). Temperature sequence: 40 °C for 17.5 h and 100 °C for 6.0 h. The positions and numbers of both monomer unit beads are not accurate, but are provided for illustrative purposes.

100 °C, guaranteeing sequence control with good chain uniformity.

Other gradient copolymers with advanced sequence control were prepared using a bifunctional RAFT agent BiCPADB (Scheme 1). BiCPADB contains two thiocarbonylthiol groups, providing two living terminals for chain growth. Therefore, two polymeric blocks would be created simultaneously in two opposite directions during polymerization. Using this bifunctional RAFT agent, gradient copolymers with complicated sequences could be readily fabricated. The varied-temperature RAFT polymerization of MMA and FPMI mediated by BiCPADB was used as an example. As shown in Fig. 3a, polymerization at 40 °C created a homo-PMMA block during the 1st slot of 22.5 h. During the 2nd slot at 100 °C for 5.0 h, a gradient copolymer block was produced. As the living polymer grew simultaneously in two opposite directions, the homo-PMMA block was located at the centre of the polymer chain with two gradient blocks at either end, resulting in a tri-block gradient copolymer. This clear sequence was also verified by the changes in $F_{\text{inst,PMI}}$ and $F_{\text{cum,PMI}}$ with normalized chain length, as shown in Fig. 3b, where a clear block-gradient sequence was observed. The living nature of tri-block gradient copolymer formation was confirmed by SEC, which showed that the molecular weight increased with conversion, affording narrow distributions (Fig. 3c). These results confirmed that a uniform tri-block gradient sequence had been fabricated. Using the same RAFT agent, polymerization was performed at 100 °C only, affording a symmetrical gradient, as shown in Fig. S9 and S10

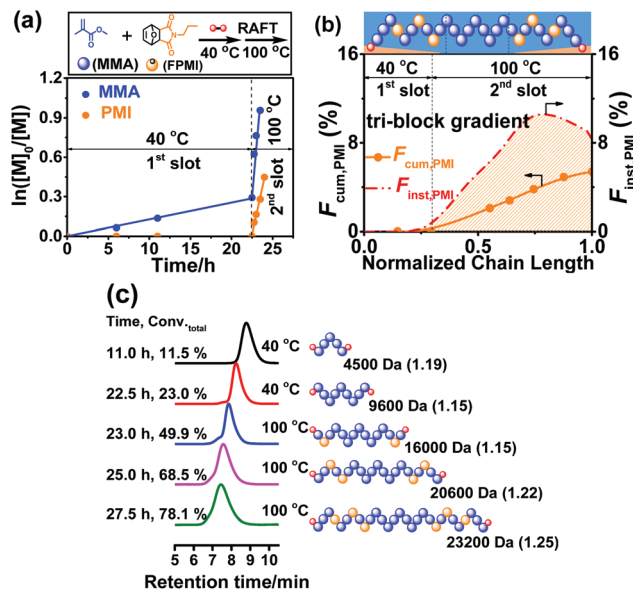


Fig. 3 Synthesis of MMA/PMI tri-block gradient copolymers using BiCPADB as the RAFT agent: (a) kinetic plots; (b) cumulative (F_{cum}) and instantaneous (F_{inst}) PMI unit contents in products as a function of normalized chain length; and (c) SEC traces. $[\text{MMA}]_0/[\text{FPMI}]_0/[\text{BiCPADB}]_0/[\text{ABVN}]_0 = 200/20/1/0.2$, $\text{MMA} = 5.0 \text{ mL}$, in toluene, toluene/MMA (1/1, v/v). Temperature sequence: 40 °C for 22.5 h and 100 °C for 5.0 h. The positions and numbers of both monomer unit beads are not accurate, but are provided for illustrative purposes.

(ESI†). An array of other advanced gradient polymers was also successfully fabricated by significantly increasing the FPMI loading ($[\text{MMA}]_0/[\text{FPMI}]_0 = 200/100$) to enable a greater incorporation of PMI (Fig. S11–S13†) into the copolymer. By employing benzyl methacrylate (BzMA) as a comonomer instead of MMA, advanced gradient polymers were prepared in a similar manner (Fig. S14 and S15†), demonstrating the universality of this methodology. The above results clearly showed that a variety of gradient copolymers with sequence control could be readily fabricated on demand in a nonintrusive manner by employing furan-protected maleimide as a comonomer. These results will greatly enrich the library of gradient polymers, help advance sequence-controlled polymerization, and facilitate research into polymer structure–property relationships.

It is envisioned that different MMA/PMI advanced gradient copolymers might convey different properties depending on the different positions of MMA and PMI units in the polymer chain.^{16,33,77} The incorporation of maleimide units into PMMA chains would elevate the glass transition temperature (T_g) and thermal stability.^{78–81} In this work, the T_g and thermal stability of different advanced gradient copolymers were explored (Fig. S16†). As shown in Table 1, the incorporation of PMI units into PMMA chains significantly enhanced both the T_g and onset temperature of decomposition (T_{d5}). Higher PMI contents afforded higher T_g s, irrespective of the type of gradient. For example, for the hierarchical, tri-block, symmetrical, and simultaneous gradient copolymers with similar molecular weights ($\sim 21\,000 \text{ Da}$) and PMI contents ($\sim 5.6\text{--}8.0\%$), the T_g s

Table 1 Thermal properties of MMA/PMI advanced gradient polymers

Samples	M_n^a (Da)	$F_{\text{cum, PMI}}^b$ (%)	T_g^c (°C)	T_{d5}^d (°C)
PMMA	20 800	0	99.7	243.0
Di-block gradient	20 000	2.7	103.3	270.2
Hierarchical gradient	21 400	5.6	118.9	334.7
Tri-block gradient	21 600	8.0	119.4	316.8
Symmetrical gradient	21 400	6.99	117.8	335.4
Simultaneous gradient	21 300	6.1	117.8	335.2
Simultaneous gradient-1	20 300	36.4	122.8	350.0
PPII	5200	100	174.0	348.0

^a Determined by SEC in THF with a PMMA standard calibration.

^b Cumulative PMI content ($F_{\text{cum, PMI}}$) determined by ^1H NMR. ^c Glass transition temperature (T_g) was determined by differential scanning calorimetry. ^d Onset temperature of decomposition (T_{d5}) was determined as the 5% weight loss temperature in thermogravimetric curves.

were found to be similar.^{33,77} A relatively low amount of PMI units in the polymer chain was possibly responsible for similar glass transition behaviour. However, regarding the thermal stability, the tri-block gradient copolymer exhibited a T_{d5} (316.8 °C) almost 20 °C lower than those of the hierarchical, symmetrical, and simultaneous gradient copolymers (around 335 °C). This might be attributed to the existence of the homo-PMMA block in the tri-block gradient copolymer, which significantly reduced the thermal stability. However, further understanding of this issue is required, which has motivated us to synthesize more advanced gradient copolymers on demand in future work.

In this work, unprecedented and tailorable advanced gradient polymers were fabricated *via* nonintrusive RAFT polymerization using FPMI as a comonomer. Polymerizable PMI can be gradually released *in situ* *via* the rDA reaction of FPMI at 100 °C to copolymerize with MMA in a gradient fashion. At low temperature, such as 40 °C, the rDA reaction for the release of maleimide could not be triggered. Herein, diverse advanced gradient copolymers, including simultaneous, hierarchical, di-block, symmetrical, and tri-block gradient polymers, were easily prepared by changing the polymerization temperature and/or employing a bifunctional RAFT agent. This work enriches the library of gradient and sequence-controlled polymers, which will advance research into the structure–property relationships and practical applications of exquisitely controlled polymers.

Conflicts of interest

There are no conflicts to declare.

Acknowledgements

Financial support from the National Nature Science Foundation of China (21674072) and the Priority Academic Program Development of Jiangsu Higher Education Institutions (PAPD) is gratefully acknowledged.

Notes and references

- 1 T. Pakula and K. Matyjaszewski, *Macromol. Theory Simul.*, 1996, **5**, 987–1006.
- 2 A. Aksimentiev and R. Holyst, *J. Chem. Phys.*, 1999, **111**, 2329–2339.
- 3 K. R. Shull, *Macromolecules*, 2002, **35**, 8631–8639.
- 4 M. K. Gray, H. Y. Zhou, S. T. Nguyen and J. M. Torkelson, *Polymer*, 2004, **45**, 4777–4786.
- 5 J. Kim, M. K. Gray, H. Y. Zhou, S. T. Nguyen and J. M. Torkelson, *Macromolecules*, 2005, **38**, 1037–1040.
- 6 K. Matyjaszewski, M. J. Ziegler, S. V. Arehart, D. Greszta and T. Pakula, *J. Phys. Org. Chem.*, 2000, **13**, 775–786.
- 7 M. K. Gray, H. Y. Zhou, S. T. Nguyen and J. M. Torkelson, *Macromolecules*, 2004, **37**, 5586–5595.
- 8 K. Matyjaszewski, *J. Macromol. Sci., Part A: Pure Appl. Chem.*, 1997, **34**, 1785–1801.
- 9 H. I. Lee, K. Matyjaszewski, S. Yu and S. S. Sheiko, *Macromolecules*, 2005, **38**, 8264–8271.
- 10 K. Karky, E. Pere, C. Pouchan, H. Garay, A. Khoukh, J. Francois, J. Desbrieres and L. Billon, *New J. Chem.*, 2006, **30**, 698–705.
- 11 L. Wang and L. J. Broadbelt, *Macromolecules*, 2010, **43**, 2228–2235.
- 12 F. Ercole, N. Malic, S. Harrison, T. P. Davis and R. A. Evans, *Macromolecules*, 2010, **43**, 249–261.
- 13 D. Neugebauer, Y. Zhang and T. Pakula, *J. Polym. Sci., Part A: Polym. Chem.*, 2006, **44**, 1347–1356.
- 14 A. S. Brar and S. Kaur, *Polym. J.*, 2005, **37**, 316–323.
- 15 Y. Ogura, T. Terashima and M. Sawamoto, *Polym. Chem.*, 2017, **8**, 2299–2308.
- 16 Y. Ogura, M. Artar, A. R. A. Palmans, M. Sawamoto, E. W. Meijer and T. Terashima, *Macromolecules*, 2017, **50**, 3215–3223.
- 17 N. G. Engeli, A. Anastasaki, G. Nurumbetov, N. P. Truong, V. Nikolaou, A. Shegiwal, M. R. Whittaker, T. P. Davis and D. M. Haddleton, *Nat. Chem.*, 2017, **9**, 171–178.
- 18 G. Gody, R. Barbey, M. Danial and S. Perrier, *Polym. Chem.*, 2015, **6**, 1502–1511.
- 19 G. Gody, T. Maschmeyer, P. B. Zetterlund and S. Perrier, *Nat. Commun.*, 2013, **4**, 2505.
- 20 M. Tesch, J. A. Hepperle, H. Klaasen, M. Letzel and A. Studer, *Angew. Chem., Int. Ed.*, 2015, **54**, 5054–5059.
- 21 C. Subramani, N. Cengiz, K. Saha, T. N. Gevrek, X. Yu, Y. Jeong, A. Bajaj, A. Sanyal and V. M. Rotello, *Adv. Mater.*, 2011, **23**, 3165–3169.
- 22 M. L. McKee, P. J. Milnes, J. Bath, E. Stulz, A. J. Turberfield and R. K. O'Reilly, *Angew. Chem., Int. Ed.*, 2010, **49**, 7948–7951.
- 23 Z. J. Gartner and D. R. Liu, *J. Am. Chem. Soc.*, 2001, **123**, 6961–6963.
- 24 J. F. Lutz, *Acc. Chem. Res.*, 2013, **46**, 2696–2705.
- 25 J. C. Barnes, D. J. C. Ehrlich, A. X. Gao, F. A. Leibfarth, Y. Jiang, E. Zhou, T. F. Jamison and J. A. Johnson, *Nat. Chem.*, 2015, **7**, 810–815.
- 26 Y. Jiang, M. R. Golder, H. V. T. Nguyen, Y. Wang, M. Zhong, J. C. Barnes, D. J. C. Ehrlich and J. A. Johnson, *J. Am. Chem. Soc.*, 2016, **138**, 9369–9372.
- 27 R. Kakuchi, *Angew. Chem., Int. Ed.*, 2014, **53**, 46–48.
- 28 F. A. Leibfarth, J. A. Johnson and T. F. Jamison, *Proc. Natl. Acad. Sci. U. S. A.*, 2015, **112**, 10617–10622.
- 29 P. J. Milnes, M. L. McKee, J. Bath, L. Song, E. Stulz, A. J. Turberfield and R. K. O'Reilly, *Chem. Commun.*, 2012, **48**, 5614–5616.
- 30 J. Xu, C. Fu, S. Shanmugam, C. J. Hawker, G. Moad and C. Boyer, *Angew. Chem., Int. Ed.*, 2017, **56**, 8376–8383.
- 31 N. F. König, A. Al Ouahabi, S. Poyer, L. Charles and J.-F. Lutz, *Angew. Chem., Int. Ed.*, 2017, **56**, 7297–7301.
- 32 S. C. Solleder, R. V. Schneider, K. S. Wetzel, A. C. Boukis and M. A. R. Meier, *Macromol. Rapid Commun.*, 2017, **38**, 1600711.
- 33 T. Soejima, K. Satoh and M. Kamigaito, *J. Am. Chem. Soc.*, 2016, **138**, 944–954.
- 34 R. B. Merrifield, *J. Am. Chem. Soc.*, 1963, **85**, 2149–2154.
- 35 S. C. Solleder, D. Zengel, K. S. Wetzel and M. A. Meier, *Angew. Chem., Int. Ed.*, 2016, **55**, 1204–1207.
- 36 M. Porel, D. N. Thornlow, N. N. Phan and C. A. Alabi, *Nat. Chem.*, 2016, **8**, 590–596.
- 37 Y. Hibi, M. Ouchi and M. Sawamoto, *Nat. Commun.*, 2016, **7**, 11064.
- 38 Z. Zhang, Y. Z. You, D. C. Wu and C. Y. Hong, *Macromolecules*, 2015, **48**, 3414–3421.
- 39 J. F. Lutz, M. Ouchi, D. R. Liu and M. Sawamoto, *Science*, 2013, **341**, 1238149.
- 40 J.-F. Lutz and H. G. Boerner, *Prog. Polym. Sci.*, 2008, **33**, 1–39.
- 41 A. H. Soeriyadi, C. Boyer, F. Nystroem, P. B. Zetterlund and M. R. Whittaker, *J. Am. Chem. Soc.*, 2011, **133**, 11128–11131.
- 42 C. Fu, J. Xu, L. Tao and C. Boyer, *ACS Macro Lett.*, 2014, **3**, 633–638.
- 43 N. Baradel, S. Fort, S. Halila, N. Badi and J.-F. Lutz, *Angew. Chem., Int. Ed.*, 2013, **52**, 2335–2339.
- 44 R. K. Roy and J.-F. Lutz, *J. Am. Chem. Soc.*, 2014, **136**, 12888–12891.
- 45 R. K. Roy, A. Meszynska, C. Laure, L. Charles, C. Verchin and J.-F. Lutz, *Nat. Commun.*, 2015, **6**, 7237.
- 46 B. K. Denizli, J. F. Lutz, L. Okrasa, T. Pakula, A. Guner and K. Matyjaszewski, *J. Polym. Sci., Part A: Polym. Chem.*, 2005, **43**, 3440–3446.
- 47 J. F. Lutz, N. Jahed and K. Matyjaszewski, *J. Polym. Sci., Part A: Polym. Chem.*, 2004, **42**, 1939–1952.
- 48 K. Nakatani, T. Terashima and M. Sawamoto, *J. Am. Chem. Soc.*, 2009, **131**, 13600–13601.
- 49 K. Nakatani, Y. Ogura, Y. Koda, T. Terashima and M. Sawamoto, *J. Am. Chem. Soc.*, 2012, **134**, 4373–4383.
- 50 Y. Ogura, T. Terashima and M. Sawamoto, *ACS Macro Lett.*, 2013, **2**, 985–989.
- 51 S. Ida, M. Ouchi and M. Sawamoto, *J. Am. Chem. Soc.*, 2010, **132**, 14748–14750.
- 52 Y. Hibi, M. Ouchi and M. Sawamoto, *Angew. Chem.*, 2011, **123**, 7572–7575.

- 53 S. Ida, M. Ouchi and M. Sawamoto, *Macromol. Rapid Commun.*, 2011, **32**, 209–214.
- 54 Y. Hibi, S. Tokuoka, T. Terashima, M. Ouchi and M. Sawamoto, *Polym. Chem.*, 2011, **2**, 341–347.
- 55 M. Matsuda, K. Satoh and M. Kamigaito, *J. Polym. Sci., Part A: Polym. Chem.*, 2013, **51**, 1774–1785.
- 56 S. Srichan, D. Chan-Seng and J.-F. Lutz, *ACS Macro Lett.*, 2012, **1**, 589–592.
- 57 M. Ojika, K. Satoh and M. Kamigaito, *Angew. Chem.*, 2017, **129**, 1815–1819.
- 58 S. Matsumoto, A. Kanazawa, S. Kanaoka and S. Aoshima, *J. Am. Chem. Soc.*, 2017, **139**, 7713–7716.
- 59 Y. Kametani, M. Nakano, T. Yamamoto, M. Ouchi and M. Sawamoto, *ACS Macro Lett.*, 2017, **6**, 754–757.
- 60 M. Ouchi, M. Nakano, T. Nakanishi and M. Sawamoto, *Angew. Chem.*, 2016, **128**, 14804–14809.
- 61 N. G. Engeli, A. Anastasaki, G. Nurumbetov, N. P. Truong, A. Shegiwal, M. R. Whittaker, T. P. Davis and D. M. Haddleton, *Nat. Chem.*, 2016, **9**, 171–178.
- 62 P. B. Zetterlund, G. Gody and S. Perrier, *Macromol. Theory Simul.*, 2014, **23**, 331–339.
- 63 G. Gody, P. B. Zetterlund, S. Perrier and S. Harrisson, *Nat. Commun.*, 2016, **7**, 10514.
- 64 Y. Ji, L. Zhang, X. Gu, W. Zhang, N. Zhou, Z. Zhang and X. Zhu, *Angew. Chem., Int. Ed.*, 2017, **56**, 2328–2333.
- 65 S. Banerjee, V. Ladmiral, A. Debuigne, C. Detrembleur, S. M. W. Rahaman, R. Poli and B. Ameduri, *Macromol. Rapid Commun.*, 2017, **38**, 1700203.
- 66 T. Oishi, M. Iwahara and M. Fujimoto, *Polym. J.*, 1991, **23**, 1409–1417.
- 67 J. Lokaj and J. Bila, *Acta Polym.*, 1992, **43**, 54–57.
- 68 T. Oishi and M. Fujimoto, *J. Polym. Sci., Part A: Polym. Chem.*, 1992, **30**, 1821–1830.
- 69 T. Oishi, K. Kagawa and M. Fujimoto, *Macromolecules*, 1993, **26**, 24–29.
- 70 R. Bharel, V. Choudhary and I. K. Varma, *J. Appl. Polym. Sci.*, 1994, **54**, 2165–2170.
- 71 K. Kagawa and T. Oishi, *Polym. J.*, 1995, **27**, 579–590.
- 72 V. Choudhary and A. Mishra, *J. Appl. Polym. Sci.*, 1996, **62**, 707–712.
- 73 K. Min, M. Li and K. Matyjaszewski, *J. Polym. Sci., Part A: Polym. Chem.*, 2005, **43**, 3616–3622.
- 74 P. H. M. Van Steenberge, D. R. D'hooge, Y. Wang, M. J. Zhong, M. F. Reyniers, D. Konkolewicz, K. Matyjaszewski and G. B. Marin, *Macromolecules*, 2012, **45**, 8519–8531.
- 75 G. F. Zhang, Q. H. Zhang, Q. Y. Wang, X. L. Zhan and F. Q. Chen, *J. Appl. Polym. Sci.*, 2016, **133**, 42936.
- 76 J. Brandrup, E. H. Immergut and E. A. Grulke, *Polymer Handbook*, Wiley-Interscience, Hoboken, 4th edn, 1993.
- 77 T. Soejima, K. Satoh and M. Kamigaito, *ACS Macro Lett.*, 2015, **4**, 745–749.
- 78 T. Otsu, A. Matsumoto, T. Kubota and S. Mori, *Polym. Bull.*, 1990, **23**, 43–50.
- 79 S. Matui and H. Aida, *Polymer*, 1976, **17**, 199–204.
- 80 S. Beppu, H. Hotta, H. Shafiee, A. Tagaya and Y. Koike, *Appl. Opt.*, 2015, **54**, 779–788.
- 81 T. Morishita, M. Matsushita, Y. Katagiri and K. Fukumori, *Carbon*, 2010, **48**, 2308–2316.